iScience

CellPress
OPEN ACCESS

Article

Smilodon fatalis siblings reveal life history in a saber-toothed cat

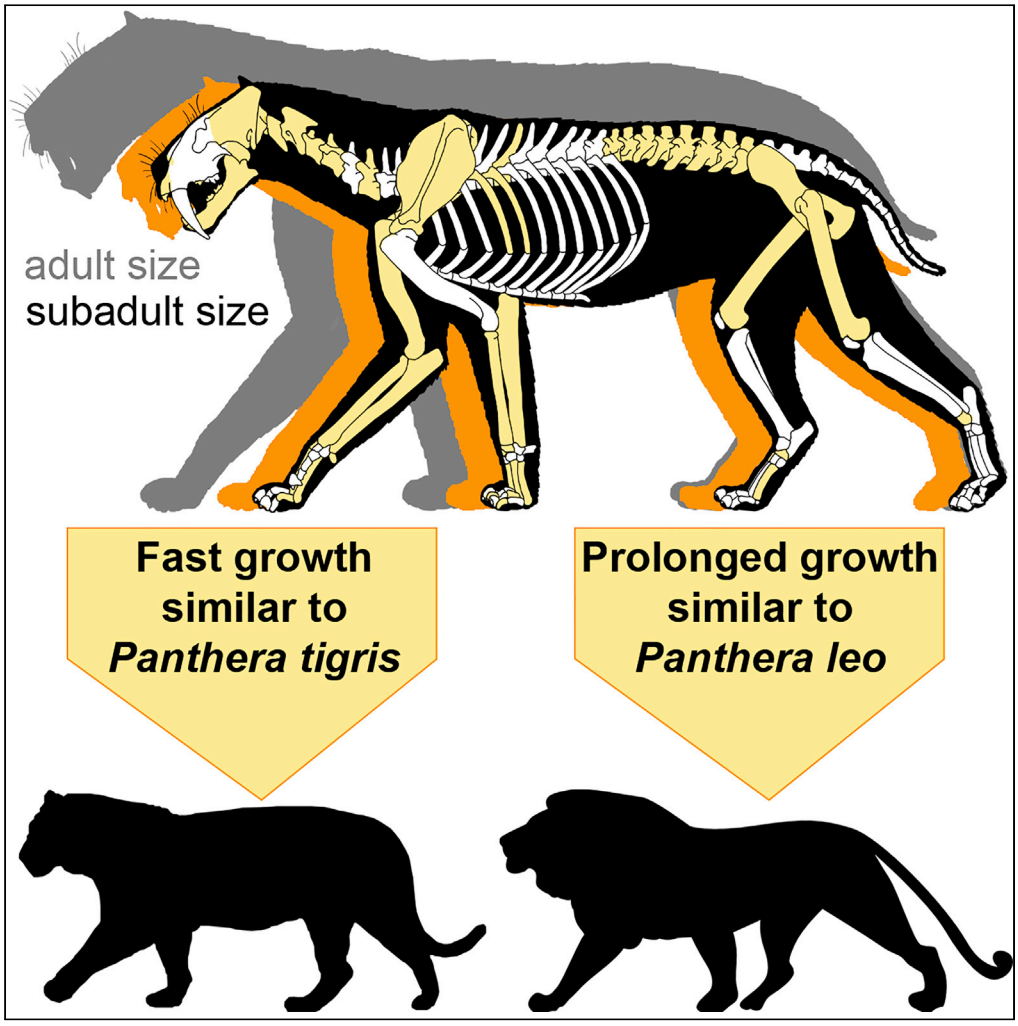

Ashley R. Reynolds, Kevin L. Seymour, David C. Evans

ashley.reynolds@mail.utoronto.ca

HIGHLIGHTS

Association of two subadult and one adult *Smilodon fatalis* from Ecuador

Rare, likely genetic condition suggests subadults are siblings

S. fatalis appears to have exhibited fast growth over a prolonged period

Comparison with growth in lions and tigers suggests a unique growth strategy

Reynolds et al., iScience *24*, 101916
January 22, 2020
https://doi.org/10.1016/j.isci.2020.101916

iScience

CellPress
OPEN ACCESS

Article

Smilodon fatalis siblings reveal life history in a saber-toothed cat

Ashley R. Reynolds,[1,2,3,*] Kevin L. Seymour,[1] and David C. Evans[1,2]

SUMMARY

The saber-toothed cat *Smilodon fatalis* is known predominantly from "predator trap" deposits, which has made many aspects of its life history difficult to infer. Here, we describe an association of at least two subadult and one adult *S. fatalis* from Pleistocene coastal deposits in Ecuador. The assemblage likely derived from a catastrophic mass mortality event, and thereby provides insights into the behavior of the species. The presence of a P_3 in the subadult dentaries suggests inheritance, a rare instance of familial relatedness in the fossil record. The siblings were at least two years old and were associated with an adult that was likely their mother, indicating prolonged parental care in *S. fatalis*. Comparison with the growth of pantherine cats suggests that *S. fatalis* had a unique growth strategy among big cats that combines a growth rate that is similar to a tiger and the extended growth period of a lion.

INTRODUCTION

The saber-toothed cat *Smilodon* occurred throughout North America and South America during the Pleistocene (Kurtén and Werdelin (1990); Reynolds et al. (2019); Rincón et al. (2011)). Of the three recognized species, *S. fatalis* is the most completely known, with thousands of well-preserved specimens in collections from asphalt seep deposits (="tar pits") (Miller (1968); Seymour (2015); Seymour et al. (2018)). While often a component of fossil assemblages from non-asphaltic depositional settings, it is frequently represented only by limited material at these localities (Kurtén and Anderson (1980); Scott and Springer (2016)). Asphalt seeps containing this iconic predator, like the ones at Rancho La Brea, California (minimum number of individuals [MNI] > 2,100) and Talara, Peru (MNI = 24), are interpreted as "predator traps" because they typically contain a disproportionate amount of material from carnivorans compared to other fossiliferous deposits (Stock and Harris (2001)). Given the attritional and time-averaged nature of tar seeps, as well as skeletal disarticulation and other signs of reworking, it is virtually impossible to identify associated individuals or even multiple bones from single individuals. Hypotheses regarding the life history and social strategy of *S. fatalis* are largely based on data collected from the Rancho La Brea asphalt seep, a predator trap, and therefore often yield conflicting conclusions. For example, high levels of sociality in *S. fatalis* have been considered plausible by some authors (Akersten (1985); Carbone et al. (2009); Christiansen and Harris (2012); Friscia et al. (2008); Gonyea (1976); Meachen-Samuels and Binder (2010); Van Valkenburgh and Sacco (2002)), but unlikely by others (Kiffner (2009); McCall et al. (2003)). Furthermore, it has been argued that *S. fatalis* would not have lived in polygynous groupings because of its putative reduced sexual dimorphism, but the possibility of social groups where polygamy or monogamy are the primary mating system cannot be discounted (Christiansen and Harris (2012); Meachen-Samuels and Binder (2010); Van Valkenburgh and Sacco (2002)).

Without the necessary evidence to determine associations between individuals of *S. fatalis* due to reworking and time-averaging, inferences about social behavior are exceptionally difficult to infer from such "predator trap" deposits. Thus, smaller fossil assemblages of associated individuals preserved in fluviodeltaic depositional environments may be more useful for inferring aspects of life history and social behavior in these carnivores (Brinkman et al. (2007); Eberth et al. (2007); Lindsey et al. (2020)). Here, we describe a multiple individual association of *Smilodon fatalis* preserved in a fluviodeltaic depositional setting at Coralito, Ecuador. Our taphonomic analysis suggests that this assemblage is best interpreted as a part of a family group derived from a catastrophic mass death event, and thereby provides unique insights into the life history of this iconic predator.

[1]Department of Natural History, Royal Ontario Museum, 100 Queen's Park, Toronto, ON M5S 1C6, Canada

[2]Department of Ecology and Evolutionary Biology, University of Toronto, 25 Willcocks Street, Toronto, ON M5S 3B2, Canada

[3]Lead Contact

*Correspondence: ashley.reynolds@mail.utoronto.ca

https://doi.org/10.1016/j.isci.2020.101916

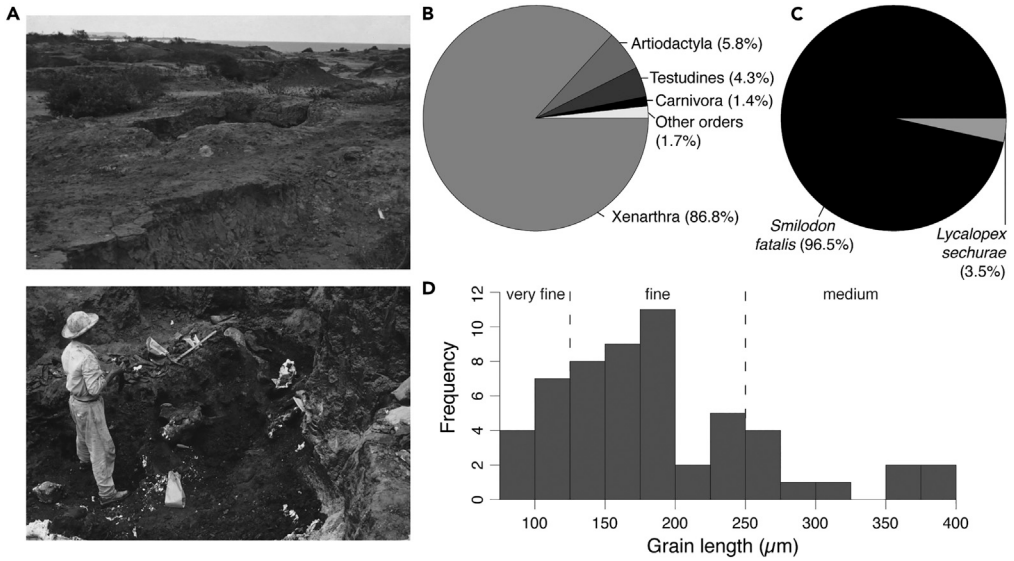

Figure 1. The Coralito locality

(A) Photographs of the Coralito locality taken during fieldwork in 1961.

(B) Pie chart showing relative representation of vertebrate specimens from Coralito, based on number of individual specimens (NISPs).

(C) Pie chart showing relative representation of carnivoran specimens from Coralito, based on NISP. Note the dominance of *Smilodon fatalis* in the carnivoran assemblage.

(D) Histogram of the grain lengths of sediment recovered from the *S. fatalis* braincase, ROMVP 5099. Dashed lines indicate breaks between very fine-, fine-, and medium-grained sand.

RESULTS

Geology and taphonomy

The Quaternary deposits of the Santa Elena Peninsula have been attributed to the Tablazo Formation (Higley (2004); Lindsey and Lopez, (2015)). The formation was deposited during Pleistocene sea-level change and tectonic uplift and is characterized by one to four wave-cut marine terraces, or tablazos (Edmund (1965); Ficcarelli et al. (2003); Marchant (1961); Pedoja et al. (2006)). Edmund (Edmund (1965) indicated that Coralito was situated on the lowest of three tablazos, at an elevation of 25 ft (7.6 m) above today's sea level, and this corresponds well with the lowest marine terrace described by other authors (Ficcarelli et al. (2003); Iriondo (1994); Pedoja et al. (2006)). Edmund (unpublished field notes, 1961) reported that the bone layer was hosted within an asphaltic sandstone lens approximately ten feet long, one and a half feet deep, and a maximum width of six feet thinning to three feet at the ends. We interpret this lenticular sandstone deposit as a small coastal channel, which is consistent with the marine signature of associated fauna, including shells, shark teeth, and turtle (Lindsey and Seymour (2015)). The source of the hydrocarbons present at the site has been hypothesized to be Tertiary shales but may derive from mid-Cretaceous shales of the Calentura Formation (Higley (2004)). The fossiliferous sediments at Coralito were tar-soaked but based on faunal composition and sedimentology have been previously interpreted as being estuarine sediments saturated with tar only after the primary deposition of the fossils (Lindsey and Seymour (2015)). Sediments recovered from inside the *S. fatalis* cranium are a fine-grained (189 $\pm$ 74 μm) sand, which is moderately sorted and sub-mature to immature. These sedimentological results suggest the Coralito deposit is most similar to Stratum V at the nearby Tanque Loma site, described by Lindsey and Lopez (Lindsey and Lopez, (2015)) as a compact, silty sandstone saturated with asphalt. Their analysis indicated the presence of relatively common 5-20 cm cobbles in this stratum; although these clasts are not present in the sediment from inside the braincase, Edmund's field notes (1961) noted that many pebbles and water-worn shells were found amongst the bones. Additionally, taphonomic indicators suggest that the death assemblage was reworked into the coastal channel shortly after the animals died (see below).

The Coralito bonebed is multitaxic and dominated by bones of large mammals. The 56 *Smilodon* bones recovered from Coralito represent 1.3% of the total number of specimens (N = 4,231) collected from the site and over 95% of the recovered carnivoran material (Figures 1B and 1C). The other carnivoran material consists of a dentary and deciduous premolar from *Lycalopex* (= *Dusicyon*) *sechurae*. It should be noted

that, while *Lutra* has been previously reported from Coralito (Lindsey and Seymour (2015)), this species was actually recovered from Rio Engabao, a locality also on the Santa Elena Peninsula of Ecuador (Edmund (1965)). This error has been corrected in the ROMVP records. The majority of material collected from Coralito is from the orders Xenarthra (86.8%), Artiodactyla (5.8%), Testudines (4.3%), and Carnivora (1.3%); the remaining orders identified from the site each represent <1% of the material. The predominance of herbivores stands in stark contrast to the composition of Talara and Rancho La Brea, where carnivorans dominate due to the predator trap nature of vertebrate accumulation at these sites.

Generally, the quality of preservation of elements is high. Of the *S. fatalis* elements collected from Coralito, 58% are categorized as having Stage 0 weathering, 29% as showing stage 0-1 weathering, and 13% as exhibiting stage 1 weathering. Abrasion is typically minimal to light, with 20% exhibiting no abrasion, 36% minimal abrasion, 35% light abrasion, and 9% moderate abrasion. Most fragile elements are broken, but numerous free epiphyses for the major limb elements were recovered and could be associated with the diaphysis of the respective element. Tooth, gnaw, and other marks are absent on the bones. Overall, cranial and thoracic limb elements are overrepresented in this sample ($N_{observed} - N_{expected}$ = 1.5% and 10.3%, respectively), while axial and pelvic limb elements are underrepresented ($N_{observed} - N_{expected}$ = −5.0% and −6.9%). Voorhies groups I and I-II are underrepresented in the sample of *Smilodon* elements ($N_{observed} - N_{expected}$ = −8.3% and −8.5%, respectively), while groups II and III are overrepresented ($N_{observed} - N_{expected}$ = 9.5% and 5.6%, respectively). The underrepresentation of smaller bones including caudal vertebrae, sternebrae, ribs, and phalanges is not unusual, given that these elements are easily broken or transported, and is consistent with an interpretation of hydrologic action (e.g., winnowing) prior to final burial (Voorhies (1969)). Cervical and lumbar vertebrae are quite well-represented compared to the remaining axial elements. Field notes by A. G. Edmund (1961) focused primarily on the herbivore remains, but he mentioned that at least some of the *Smilodon* elements at this locality were found together early in the field season; for example, he noted recovering one of the two dentaries alongside a premaxilla (ROMVP 5102).

Although we only document the taphonomic stages of the *Smilodon* bones, the majority of the bones in the deposit exhibit the same stages of weathering, abrasion, and breakage as noted above, suggesting that the deposit likely represents a reworked mass death assemblage (Rogers et al. (2007)). Given the small size of the fossiliferous deposits at Coralito, low variation in taphonomic indicators across most elements, and the close association of the *Smilodon* elements recovered, it is likely that the subadults described here died together, perhaps as part of a larger catastrophic mass kill mechanism.

Description and ontogenetic assessment

Of the 56 felid bones recovered from the site, most of these specimens are postcranial (N = 52, 92.9%), but cranial material includes a braincase, premaxilla, and two dentaries (Figures 2A–2C and 3). Comparisons of all material with ROMVP *Smilodon fatalis* material from the nearby locality of Talara, Peru (Seymour et al. (2018)) indicates that all felid material can be assigned to that species. A full list and description of the material here ascribed to *S. fatalis*, as well as measurements for this material, can be found in the Electronic Supplementary Material (Supplemental Information, Table S1 and Systematic Palaeontology). Only a single duplication of elements, two left dentaries (ROMVP 5100 and ROMVP 5101; Figure 3) is present, despite the fact that all of the material pertains to a similarly sized subadult individual. A single right ulna (ROMVP 5108; Figure 2D) is adult, based on epiphyseal fusion, and this element is much larger than would be expected given the size of the cranial material. Since ROMVP 5108 is too large to belong with the two dentaries, the minimum number of *S. fatalis* individuals at this locality is three.

The cranial material (two left dentaries, a right premaxilla, isolated P^3, and braincase; Figures 2A–2C and 3) is derived from young adult individuals based on the presence of a fused basioccipital-basisphenoid suture (ROMVP 5099) and a full complement of erupted adult dentition with minimal tooth wear (ROMVP 5100, ROMVP 5101, ROMVP 5102, and ROMVP 5103). The skull, ROMVP 5099 (Figure 2C), can be readily identified as *Smilodon fatalis* because of its large, anteriorly projecting mastoid process that has an obtuse angle relative to the lambdoid crest (Kurtén and Werdelin (1990); Merriam and Stock (1932)). The two dentaries, ROMVP 5100 and ROMVP 5101 (Figure 3), are remarkably similar in size (total length for ROMVP 5100 is 194.1 mm and for ROMVP 5101 is 197.0 mm), suggesting that the remainder of the subadult material likely came from a combination of these two individuals, but they cannot reliably be differentiated. The small canines, low coronoid process, and lateral flanges are consistent with a machairodontine cat (Merriam and Stock (1932)). The reduced mandibular flange suggests the dentaries belong to the genus *Smilodon*

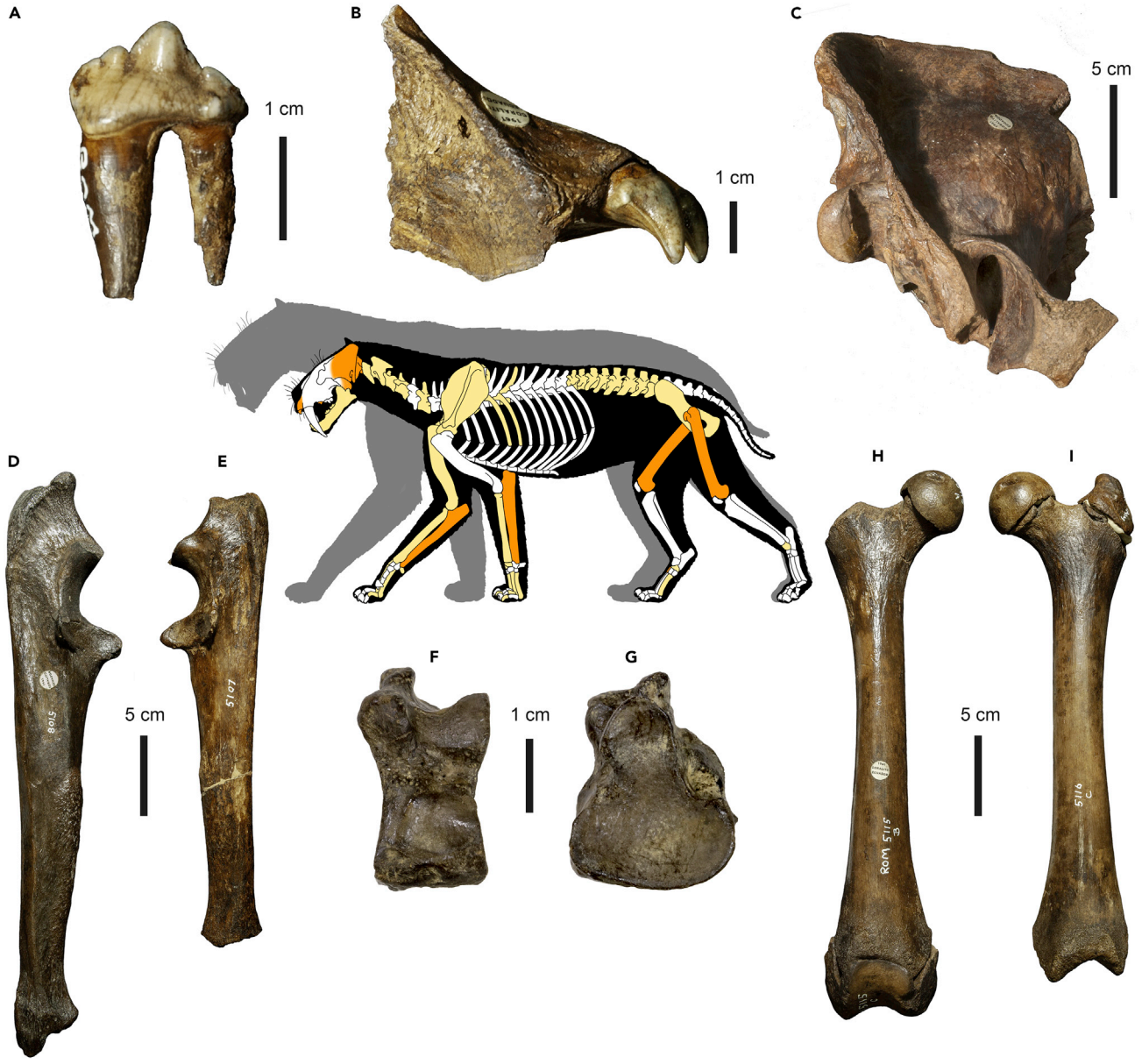

Figure 2. *Smilodon fatalis* material recovered from Coralito

Colored elements in the skeletal reconstruction indicate elements present in the assemblage, with the elements figured highlighted in orange. The gray silhouette behind the skeletal reconstruction represents the relative body size of the adult specimen, represented by an ulna (ROMVP 5108), compared with the subadult material. Skeletal reconstruction provided by Scott Hartman.

(A) Right P^3, ROMVP 5103, buccal view.

(B) Right premaxilla with I^2 and I^3, ROMVP 5102, lateral view.

(C) Braincase, ROMVP 5099, right lateral view.

(D) Adult right ulna, ROMVP 5108, lateral view.

(E) Subadult left ulna, ROMVP 5107, lateral view.

(F) Right ectocuneiform, ROMVP 19296, medial view.

(G) Right ectocuneiform, ROMVP 19296, proximal view.

(H) Right subadult femur, ROMVP 5115, anterior view.

(I) Left subadult femur, ROMVP 5116, anterior view.

See also Tables S1 and S2.

Figure 3. Comparison of the two left dentaries, ROMVP 5100 and ROMVP 5101

All views use the same scale.

(A) ROMVP 5100 in occlusal (top) and lateral (bottom) view.

(B) ROMVP 5101 in occlusal (top) and lateral (bottom) view. Note the slightly longer total length and relatively longer M_1 in this specimen.

and, while a variable character, the single mental foramen is consistent with an identification of either *S. fatalis* or *S. populator* (Berta (1985); Werdelin and Flink (2018)). Given the relatively small size of the two dentaries and that the other *Smilodon* material can be readily identified as *S. fatalis*, we assign these specimens to *S. fatalis*. Interestingly, both dentaries possess a P_3, either as broken roots only (ROMVP 5100) or with an associated tooth (ROMVP 5101). This is rare in *S. fatalis* and may be evidence of close genetic relationship between these two subadult individuals (see discussion below).

Almost all postcranial material is categorized as subadult, as evidenced by the unfused epiphyses on 94% of axial elements and 70% of major limb elements. The metapodials from this assemblage are relatively gracile compared to those from *S. populator* (see Figure 9 in Kurtén and Werdelin (Kurtén and Werdelin (1990)), in which the Coralito metatarsal II falls within *S. fatalis* morphospace in a regression of length and shaft width of this element; also see Supplemental Information, Table S2), in addition to being smaller in all dimensions relative to the Talara *S. fatalis*. The right ectocuneiform (ROMVP, 19296; Figures 2F and 2G) is of the truncated morphology that is rare at Rancho La Brea (23.8%), but relatively more common at Talara (44.5%) (Merriam and Stock (1932); Shaw and Tejada-Flores (1985)). The postcranial material overwhelmingly indicates a juvenile or subadult status, whereas the adult dentition is fully erupted in all of the known cranial elements. A disparity in the proportion of subadults based on cranial versus postcranial material is expected for two reasons. First, a similar trend can be observed among material from Talara, Peru (Seymour et al. (2018)). Second, this is observed for extant felids; the dentition of the lion, *Panthera leo*, fully erupts by 1.25–1.67 years, while the epiphyses do not fully fuse for up to 5.5 years (Kirberger et al., (2005a), (2005b); Smuts et al. (1978)). Thus, in extant lions the teeth may be fully erupted for as long as 4.25 years before the postcranial epiphyses will fully fuse.

Body size estimates based on the two subadult femora yield masses of 131.8 kg and 140.6 kg, respectively (Table 1). These estimates are 76% and 81%, respectively, of the mean estimated body mass (173.0 kg) for

Table 1. Body mass estimates for the Coralito subadults, based on femur circumference and M_1 length

Body mass estimates from femur circumference			
Specimen	Femur circumference (mm)	Body mass (kg)	% Mean Talara adult
ROMVP 5115	91	131.8	76%
ROMVP 5116	93	140.6	81%

Body mass estimates from M_1 length			
Specimen	M_1 length (mm)	Body mass (kg)	% mean Talara adult
ROMVP 5100	24.53	124.2	55%
ROMVP 5101	27.42	173.4	98%

adult Talara femora (N = 9). There is relatively more variation between the dentaries when M_1 length is used to estimate body mass (ROMVP 5100: 24.53 mm; ROMVP 5101: 27.42 mm), which yields body mass estimates of 124.1 kg and 173.4 kg, respectively. These estimates represent 55% (ROMVP 5100) and 98% (ROMVP 5101) of the mean body mass (181.8 kg) estimated for the M_1 at Talara (N = 27). However, because we could estimate sex for these two specimens, we can compare these to estimated mean body masses for previously sexed females (N = 8; 176 kg) and males (N = 2; 225 kg) from Talara (Seymour et al. (2018)). Estimates of sex following Christiansen & Harris (Christiansen and Harris (2012)) suggest that ROMVP 5100 was of the large (presumably male) morphotype, and weighed 55% of the estimated male body mass at Talara, 226.0 kg. ROMVP 5101 was of the small (presumably female) morphotype, weighing 98% of the estimated female body mass at Talara, 176.7 kg. However, we note that Christiansen and Harris (2012) did not account for the ontogenetic stage of their specimens, which may affect the results on the subadults here.

DISCUSSION

Depositional setting

Consistent taphonomic signatures from a single small deposit suggest that the vertebrate fossil material from Coralito shares a similar taphonomic history and that the individuals in the bone assemblage likely originated from a single catastrophic mass death event. Flooding of the coastal plain has been suggested as the origin for other dense bonebed accumulations deposited in similar environments (Brinkman et al. (2007); Eberth et al. (2007)). Alternatively, drought has been proposed as a mechanism of catastrophic death for other somewhat similar deposits on the Santa Elena Peninsula, in particular at Tanque Loma, which is located geographically close to Coralito (Lindsey et al. (2020)). In this scenario, megaherbivores (ground sloths) have been hypothesized to have congregated at wallowing sites, where contamination of water with fecal matter may have spread disease (Lindsey et al. (2020)). During the late Pleistocene, the region was cooler and likely more arid overall, with the lowest levels of precipitation in southwestern Ecuador occurring at ~15,000 ybp (Heusser and Shackleton (1994); Koutavas et al. (2002); Lindsey and Lopez, (2015)). However, it has also been suggested that the El Niño Southern Oscillation, which today can deliver heavy rainfalls in coastal Ecuador, was a phenomenon that was active in the region during the Pleistocene and may have caused seasonal floods (Iriondo (1994); Lindsey and Lopez, (2015)). Given the possibility of strong seasonal fluctuations between dry conditions and heavy rains, we hypothesize that one of these processes caused the mass mortality of the *Smilodon* individuals at Coralito, and those of the other taxa in the assemblage. Carcasses were exposed long enough to allow for soft tissue decay and disarticulation of the skeleton and connective tissues to decay before the largely disarticulated, yet still associated, bones were subsequently reworked into a small channel and buried as an assemblage of associated elements. The relatively low number of *Smilodon* individuals (only 1.3% of the total assemblage), the dearth of other carnivores at the site (including the dire wolf *Canis dirus*, which is more common than *S. fatalis* at Talara), the lack of tooth marks or gnaw marks on the bones, and the associated nature of material, are all consistent with an interpretation that at least three *Smilodon* individuals were living together as a social group when they died.

Relatedness of subadult individuals

Relative size and taphonomic indicators clearly suggest that the two subadult individuals in the Coralito sample are from the same cohort, with the single adult ulna representing the only mature individual in the *Smilodon* assemblage. The unusual presence of an adult P_3 premolar in both of the subadult left

dentaries strongly suggests that these two individuals are genetically related, and likely siblings. In the Rancho La Brea population of *Smilodon fatalis*, a P_3 is only present in between 2.4 and 6% of the population (Babiarz et al. (2018); McDonald and Werdelin (2018); Merriam and Stock (1932)), and the incidence of this tooth for Talara material in the ROMVP collections is within this range at 4.2%. Therefore, at these rates, the probability of randomly finding any two individuals together with an adult P_3 is exceedingly low, between 0.06 and 0.36%. Furthermore, studies on mammalian model organisms such as humans, rats, and mice suggest that non-syndromic presence or absence of teeth (i.e. with no pleiotropic conditions such as cleft palate) may be inherited (Galluccio et al. (2012)). Familial studies in humans have shown that, depending on the gene or chromosome affected and the specific type of mutation within that family, inheritance of abnormal dentitions may be X-linked, recessive autosomal, or dominant autosomal (Galluccio et al. (2012)). To our knowledge, there have been no studies on the inheritance patterns of dental presence or absence in felids. However, in domestic cats, supernumerary premolars mesial to the P^2 and P_3 have been noted to have an incidence of 3.7–4.5% (Verstraete et al. (1996); Verstraete and Terpak (1997)). Therefore, we cannot say which mode of inheritance was involved in the presence of a P_3 in some *S. fatalis* individuals, but its expression in the two subadult dentaries from Coralito is strongly suggestive of inheritance from the same parents, given the comparable size of these individuals and their identical taphonomic signatures.

Implications for life history in *Smilodon fatalis*

The presence of at least two subadult siblings with a single mature individual, which we hypothesize were killed in the same event, has implications for understanding the ecology of *Smilodon fatalis*, which has been controversial (Akersten (1985); Binder and Van Valkenburgh (2010); Carbone et al. (2009); Christiansen and Harris (2012); Gonyea (1976); Kiffner (2009); McCall et al. (2003); Meachen-Samuels and Binder (2010); Seymour et al. (2018); Van Valkenburgh and Sacco (2002)). Two scenarios are most likely for the Coralito assemblage. The first is that the subadults may have been young adolescents that were independent from their mother but still part of a sibling group, and the adult ulna is derived from an unrelated individual. Sibling groups have been observed in several large extant felids and may last for a short time, as in pumas (Seidensticker et al. (1973)), or may persist for a lifetime as in lions (Chakrabarti and Jhala (2019); Joslin (1973); Pusey and Packer (1987)) and cheetahs (Caro (1994)). If the subadults represented by ROMVP 5100 and ROMVP 5101 were independent from their mother at the time of death, this suggests that *S. fatalis* similarly formed independent sibling groups, whether transient or permanent. The second, and better supported scenario given the consistency of the taphonomic signatures between the adult ulna and subadult bones, is that the subadults were still dependent on their mother, and all were together at the time of death. This would be indicative of prolonged parental care in *S. fatalis*, which has been previously proposed based on estimates of tooth eruption (Wysocki et al. (2015)).

The permanent dentition in *S. fatalis* (aside from the C^1, for which we cannot determine the eruption status) is fully erupted by 14-22 months, so the individuals represented by the two subadult dentaries were at minimum 14 months old. Histological sampling of a two-year-old juvenile *S. fatalis* with a slightly smaller minimum femoral circumference (ROMVP 4720, 84 mm circumference (Seymour et al. (2018))) from Talara suggests that both similarly sized femora ROMVP 5115 and ROMVP 5116 came from individuals that were likewise at least two years old at death (Seymour et al. (2018)). At two years old, tigers (*Panthera tigris*) have been independent from their mothers for at least six months and weigh between 68% (males) and 94% (females) of their asymptotic body mass (Jones et al. (2009); Slaght et al., 2005). Meanwhile, two-year-old lions are nearly a year from independence and weigh from 58% (males) to 72% (females) of asymptotic body mass (Jones et al. (2009); Smuts et al. (1980)).

The femur may be a better predictor of subadult body mass than the M_1, as the former is able to actively respond to loading pressures during ontogeny and dental measurements may be impacted by sex differences, but the femora in our sample cannot be sexed. Because extant felids are sexually dimorphic in growth patterns, the postcranial elements therefore provide limited data on relative maturity based on growth curve comparisons. Additionally, it is possible that both femora belong to a single individual. We are therefore using body mass estimates generated from the M_1 here but urge caution in interpretation. The estimated body masses for ROMVP 5100 and ROMVP 5101 are 55% and 98% of the mean estimated body mass for Talara M_1. This suggests that, like living tigers, males and females matured at different rates, with females potentially reaching adult size at around two years of age. Conversely, given the presence of a relatively large adult individual in the assemblage, represented by the ulna ROMVP 5108, it is likely that these were dependent siblings and the adult ulna is from their mother. Two-year-old tigers

would be independent at this stage, so it therefore appears that *S. fatalis* had prolonged parental care more like that seen in lions. The development of the hypertrophied upper canines in *S. fatalis* has similarly been shown to exhibit a mixture of tiger- and lion-like strategies, in which growth is rapid but occurs over a prolonged period of time (Feranec (2004)). These results suggest that a combination of tiger and lion life history strategies may have evolved in *S. fatalis* more broadly, and not only in the dentition.

The coastal bonebed at Coralito provides unique insights into the life history of the iconic saber-toothed cat *Smilodon fatalis* beyond that which can be provided by tar pit predator trap assemblages. The deposit preserves at least two subadult *S. fatalis* siblings, a rare instance of post-natal familial relatedness of individuals in the mammal fossil record. The siblings were at least two years old at death and were associated with a large adult that was likely their mother, providing evidence for prolonged parental care in *S. fatalis*, similar to that of a lion. However, comparison with the growth patterns of extant lions and tigers suggests that *S. fatalis* grew more similarly to a tiger. Taken together, these data suggest that *S. fatalis* may have had a unique growth strategy that combines the faster growth rate of a tiger with the extended growth period of a lion.

Limitations of the study

Due to the historic nature of these specimens' collection, detailed *in situ* stratigraphic, sedimentological, and taphonomic information was not available to the authors. This necessitated drawing conclusions based on unpublished field notes and previously published studies of nearby localities within the same geological formation and/or in similar environments, as well as taphonomic signals on the bones themselves. Furthermore, while we believe that body mass estimates based on femur dimensions would be preferable for subadult individuals, the lack of association data prevented us from determining whether these femora belonged to one, both, or neither individual represented by a dentary, although the latter is unlikely given the lack of duplication in other elements and small depositional area. Our body mass estimates and corresponding analyses of growth patterns in *S. fatalis* may therefore have limitations. Additionally, the method used for sexing ROMVP 5100 and ROMVP 5101 do not account for ontogenetic variation, and our determinations of these specimens as male and female, respectively, must be treated as hypotheses based on the data that are currently available.

Resource availability

Lead contact

Further information and requests for information should be directed to and will be fulfilled by the Lead contact, Ashley R. Reynolds (ashley.reynolds@mail.utoronto.ca).

Materials availability

This study did not generate new unique reagents.

Data and code availability

Measurement data can be found in the Supplemental Information for this article.

METHODS

All methods can be found in the accompanying Transparent Methods supplemental file.

SUPPLEMENTAL INFORMATION

Supplemental Information can be found online at https://doi.org/10.1016/j.isci.2020.101916.

ACKNOWLEDGMENTS

We would like to thank B. Iwana for preparation of specimens in this paper and I. Morrison for the retrieval of sediment samples. We thank D. Dufault for assistance with figure design and accompanying reconstruction. Thank you to S. Hartman for the use of his skeletal reconstruction of *Smilodon*. Many thanks to V. DiCecco for assistance with sedimentological analysis. Advice on cleaning asphaltic sediments was generously provided by A. Farrell, E. Herring, E. Lindsey, and K. Rice. Thank you to D. Eberth for comments that helped improve this manuscript. Research was supported by an Ontario Graduate Scholarship to

A.R.R. and a Natural Sciences and Engineering Research Council of Canada (NSERC) Discovery Grant to D.C.E. (NSERC Grant File Number: RGPIN 355845).

AUTHOR CONTRIBUTIONS

Conceptualization: A.R.R. and D.C.E.; Methodology: A.R.R., K.L.S., and D.C.E; Validation: A.R.R.; Investigation: A.R.R. and K.L.S.; Formal Analysis: A.R.R.; Resources: K.L.S. and D.C.E; Data Curation: A.R.R.; Writing – Original Draft: A.R.R.; Writing – Review & Editing: A.R.R., K.L.S., and D.C.E.; Visualization: A.R.R. and D.C.E.; Supervision: D.C.E.; Project Administration: A.R.R. and D.C.E.; Funding Acquisition: A.R.R. and D.C.E.

DECLARATION OF INTERESTS

The authors declare no competing interests.

Received: October 20, 2020
Revised: November 18, 2020
Accepted: December 7, 2020
Published: January 7, 2021

REFERENCES

Akersten, W.A. (1985). Canine function in *Smilodon* (Mammalia; Felidae; Machairodontinae). Nat. Hist. Museum Los Angeles cty. Contrib. Sci. *356*, 1–22.

Babiarz, J.P., Wheeler, H.T., Knight, J.L., and Martin, L.D. (2018). Smilodon from South Carolina: implications for the taxonomy of the genus. In Smilodon: The Iconic Sabertooth, L. Werdelin, H.G. McDonald, and C.A. Shaw, eds. (Johns Hopkins University Press), pp. 76–107.

Berta, A. (1985). The status of *Smilodon* in North and South America. Contrib. Sci. *370*, 1–15.

Binder, W.J., and Van Valkenburgh, B. (2010). A comparison of tooth wear and breakage in Rancho La Brea sabertooth cats and dire wolves across time. J. Vertebr. Paleontol. *30*, 255–261.

Brinkman, D.B., Eberth, D.A., and Currie, P.J. (2007). From bonebeds to paleobiology: applications of bonebed data. In Bonebeds: Genesis, Analysis, and Paleobiological Significance, R.R. Rogers, D.A. Eberth, and A.R. Fiorillo, eds. (The University of Chicago Press), pp. 221–264.

Carbone, C., Maddox, T., Funston, P.J., Mills, M.G.L., Grether, G.F., and Van Valkenburgh, B. (2009). Parallels between playbacks and Pleistocene tar seeps suggest sociality in an extinct sabretooth cat, *Smilodon*. Biol. Lett. *5*, 81–85, https://doi.org/10.1098/rsbl.2008.0526.

Caro, T.M. (1994). Cheetahs of the Serengeti Plains: Group Living in an Asocial Species (The University of Chicago Press).

Chakrabarti, S., and Jhala, Y.V. (2019). Battle of the sexes: a multi-male mating strategy helps lionesses win the gender war of fitness. Behav. Ecol. *30*, 1–12.

Christiansen, P., and Harris, J.M. (2012). Variation in craniomandibular morphology and sexual dimorphism in pantherines and the sabercat *Smilodon fatalis*. PLoS One *7*, e48352.

Eberth, D.A., Rogers, R.R., and Fiorillo, A.R. (2007). A practical approach to the study of bonebeds. In Bonebeds: Genesis, Analysis, and Paleobiological Significance, R.R. Rogers, D.A. Eberth, and A.R. Fiorillo, eds. (The University of Chicago Press), pp. 265–332.

Edmund, A.G. (1965). A late pleistocene fauna from the Santa Elena Peninsula, Ecuador. R. Ontario Mus. Life Sci. Contrib. *63*, 1–21.

Feranec, R.S. (2004). Isotopic evidence of sabertooth development, growth rate, and diet from the adult canine of *Smilodon fatalis* from Rancho La Brea. Palaeogeogr. Palaeoclimatol. Palaeoecol. *206*, 303–310.

Ficcarelli, G., Coltorti, M., Moreno-Espinosa, M., Pieruccini, P.L., Rook, L., and Torre, D. (2003). A model for the Holocene extinction of the mammal megafauna in Ecuador. J. South Am. Earth Sci. *15*, 835–845.

Friscia, A.R., Van Valkenburgh, B., Spencer, L.M., and Harris, J.M. (2008). Chronology and spatial distribution of large mammal bones in pit 91, Rancho La Brea. Palaios *23*, 35–42.

Galluccio, G., Castellano, M., and La Monaca, C. (2012). Genetic basis of non-syndromic anomalies of human tooth number. Arch. Oral Biol. *57*, 918–930.

Gonyea, W.J. (1976). Behavioral implications of saber-toothed felid morphology. Palaeobiology *2*, 332–342.

Heusser, L.E., and Shackleton, N.J. (1994). Tropical climate variation on the pacific slopes of the ecuadorian andes based on a 25,000-year pollen record from deep-sea sediment core tri 163-31B. Quat. Res. *42*, 222–225.

Higley, D.K. (2004). The Progreso Basin Province of Northwestern Peru and Southwestern Ecuador: Neogene and Cretaceous-Paleogene Total Petroleum Systems (US Geological Survey Bulletin 2206-B).

Iriondo, M. (1994). The quaternary of Ecuador. Quat. Int. *21*, 101–112.

Jones, K.E., Bielby, J., Cardillo, M., Fritz, S.A., O'Dell, J., Orme, C.D.L., Safi, K., Sechrest, W., Boakes, E.H., Carbone, C., et al. (2009). PanTHERIA: a species-level database of life history, ecology, and geography of extant and recently extinct mammals. Ecology *90*, 2648.

Joslin, P. (1973). The Asiatic Lion: A Study of Ecology and Behaviour (University of Edinburgh).

Kiffner, C. (2009). Coincidence or evidence: was the sabretooth cat *Smilodon* social? Biol. Lett. *5*, 561–562.

Kirberger, R.M., du Plessis, W.M., and Turner, P.H. (2005a). Radiologic anatomy of the normal appendicular skeleton of the lion (*Panthera leo*). Part 2: pelvic limb. J. Zoo Wildl. Med. *36*, 29–35.

Kirberger, R.M., du Plessis, W.M., and Turner, P.H. (2005b). Radiologic anatomy of the normal appendicular skeleton of the lion (*Panthera leo*). Part 1: thoracic limb. J. Zoo Wildl. Med. *36*, 21–28.

Koutavas, A., Lynch-Stieglitz, J., Marchitto, T.M., and Sachs, J.P. (2002). El Niño-like pattern in ice age tropical pacific sea surface temperature. Science *297*, 226–230.

Kurtén, B., and Anderson, E. (1980). Pleistocene Mammals of North America (Columbia University Press).

Kurtén, B., and Werdelin, L. (1990). Relationships between North and South American *Smilodon*. J. Vertebr. Paleontol. *10*, 158–169.

Lindsey, E.L., and Lopez, R.E.X. (2015). Tanque Loma, a new late-Pleistocene megafaunal tar seep locality from southwest Ecuador. J. South Am. Earth Sci. *57*, 61–82.

Lindsey, E.L., Lopez Reyes, E.X., Matzke, G.E., Rice, K.A., Mcdonald, H.G., Reyes, E.X.L., Matzke, G.E., Rice, K.A., and Mcdonald, H.G. (2020). A monodominant late-Pleistocene megafauna locality from Santa Elena, Ecuador: insight on the

biology and behavior of giant ground sloths. Palaeogeogr. Palaeoclimatol. Palaeoecol. *544*, 109599.

Lindsey, E.L., and Seymour, K.L. (2015). "Tar pits" of the western neotropics: paleoecology, taphonomy, and mammalian biogeography. In La Brea and beyond: The Paleontology of Asphalt-Preserved Biotas, Natural History Museum of Los Angeles County Science Series No. 42, J.M. Harris, ed. (Allen Press, Inc.), pp. 111–123.

Marchant, S. (1961). A photogeological analysis of the structure of the western Guayas province, Ecuador: with discussion of the stratigraphy and Tablazo Formation, derived from surface mapping. Q. J. Geol. Soc. Lond. *117*, 215–231.

McCall, S., Naples, V.L., and Martin, L.D. (2003). Assessing behavior in extinct animals: was *Smilodon* social? Brain Behav. Evol. *61*, 159–164.

McDonald, H.G., and Werdelin, L. (2018). The Sabertooth Cat, *Smilodon populator* (Carnivora, Felidae), from Cueva del Milodón, Chile. In Smilodon: The Iconic Sabertooth, L. Werdelin, H.G. McDonald, and C.A. Shaw, eds. (Johns Hopkins University Press), pp. 53–75.

Meachen-Samuels, J.A., and Binder, W.J. (2010). Sexual dimorphism and ontogenetic growth in the American lion and sabertoothed cat from Rancho La Brea. J. Zool. *280*, 271–279.

Merriam, J.C., and Stock, C. (1932). The Felidae of Rancho La Brea (Carnegie Institution of Washington, Publication), p. 422.

Miller, G.J. (1968). On the age distribution of *Smilodon californicus* bovard from Rancho La Brea. Los Angeles cty. Mus. Contrib. Sci. Sci. *131*, 1–17.

Pedoja, K., Ortlieb, L., Dumont, J.F., Lamothe, M., Ghaleb, B., Auclair, M., and Labrousse, B. (2006). Quaternary coastal uplift along the Talara Arc (Ecuador, Northern Peru) from new marine terrace data. Mar. Geol. *228*, 73–91.

Pusey, A.E., and Packer, C. (1987). The evolution of sex-biased dispersal in lions. Behaviour *101*, 275–310.

Reynolds, A.R., Seymour, K.L., and Evans, D.C. (2019). Late Pleistocene records of felids from Medicine Hat, Alberta, including the first Canadian record of the sabre-toothed cat Smilodon fatalis. Can. J. Earth Sci. *56*, 1052–1060.

Rincón, A.D., Prevosti, F.J., and Parra, G.E. (2011). New saber-toothed cat records (Felidae: Machairodontinae) for the pleistocene of Venezuela, and the Great American biotic Interchange. J. Vertebr. Paleontol. *31*, 468–478.

R.R. Rogers, D.A. Eberth, and A.R. Fiorillo, eds. (2007). Bonebeds: Genesis, Analysis, and Paleobiological Significance (The University of Chicago Press).

Scott, E., and Springer, K.B. (2016). First records of *Canis dirus* and *Smilodon fatalis* from the late pleistocene tule springs local fauna, upper Las Vegas Wash, Nevada. PeerJ *4*, e2151.

Seidensticker, J.C., Hornocker, M.G., Wiles, W.V., and Messick, J.P. (1973). Mountain lion social organization in the Idaho primitive area. Wildl. Monogr. *35*, 3–60.

Seymour, K.L. (2015). Perusing Talara: overview of the late pleistocene fossils from the tar seeps of Peru, La Brea beyond Paleontol. Asph. Biotas, Nat. Hist. Museum Los Angeles Cty. Science *42*, 97–109. https://tarpits.org/sites/default/files/2019-05/la_brea_and_beyond_2015._nhm_science_science_no._42.pdf#page=100.

Seymour, K.L., Reynolds, A.R., and Churcher, C.S. (2018). *Smilodon fatalis* from Talara, Peru: sex, age, mass, and histology. In Smilodon: The Iconic Sabertooth, L. Werdelin, H.G. McDonald, and C.A. Shaw, eds. (Johns Hopkins University Press), pp. 30–52.

Shaw, C.A., and Tejada-Flores, A.E. (1985). Biomechanical implications of the variation in Smilodon ectocuneiforms from Rancho La Brea. Los Angeles cty. Mus. Contrib. Sci. *359*, 1–8.

Slaght, J.C., Miquelle, D.G., Nikolaev, I.G., Goodrich, J.M., Smirnov, E.N., Traylor-Holzer, K., Christie, S., Arjanova, T., Smith, J.L.D., and Karanth, K.U. (2005). Chapter 6. Who's king of the beasts? Historical and recent body weights of wild and captive Amur tigers, with comparisons to other subspecies. In Tigers in Sikhote-Alin Zapovednik: Ecology and Conservation, D.G. Miquelle, E.N. Smirnov, and J.M. Goodrich, eds. (PSP), pp. 25–35.

Smuts, G.L., Anderson, J.L., and Austin, J.C. (1978). Age determination of the African lion (*Panthera leo*). J. Zool. *185*, 115–146.

Smuts, G.L., Robinson, G.A., and Whyte, I.J. (1980). Comparative growth of wild male and female lions (*Panthera leo*). J. Zool. *190*, 365–373.

Stock, C., and Harris, J.M. (2001). Rancho La Brea: A Record of Pleistocene Life in California, Seventh Edition (Natural History Museum of Los Angeles County).

Van Valkenburgh, B., and Sacco, T. (2002). Sexual dimorphism, social behavior, and intrasexual competition in large Pleistocene carnivorans. J. Vertebr. Paleontol. *22*, 164–169.

Verstraete, F.J.M., and Terpak, C.H. (1997). Anatomical variations in the dentition of the domestic cat. J. Vet. Dent. *14*, 137–140.

Verstraete, F.J.M., van Aarde, R.J., Nieuwoudt, B.A., Mauer, E., and Kassw, P.H. (1996). The dental pathology of feral cats on marion island, part i: congenital, developmental and traumatic abnormalities. J. Comp. Pathol. *115*, 265–282.

Voorhies, M.R. (1969). Taphonomy and population dynamics of an early pliocene vertebrate fauna, Knox County, Nebraska. Contrib. Geol., Univ. Wyo. Press *1*, 1–69. https://doi.org/10.2113/gsrocky.8.special_paper_1.1.

Werdelin, L., and Flink, T. (2018). The phylogenetic context of Smilodon. In Smilodon: The Iconic Sabertooth, L. Werdelin, H.G. McDonald, and C.A. Shaw, eds. (Johns Hopkins University Press), pp. 14–29.

Wysocki, M.A., Feranec, R.S., Tseng, Z.J., and Bjornsson, C.S. (2015). Using a novel absolute ontogenetic age determination technique to calculate the timing of tooth eruption in the saber-toothed cat, *Smilodon fatalis*. PLoS One *10*, e0129847.

iScience, Volume *24*

Supplemental Information

Smilodon fatalis siblings reveal life history in a saber-toothed cat

Ashley R. Reynolds, Kevin L. Seymour, and David C. Evans

Table S2. Comparative measurements of metapodials from *S. fatalis* , *S. populator* , and specimens from Coralito, Ecuador; related to Description and Ontogenetic Assessment and Figrue 2.

METACARPAL II	**ROMVP 5123**	**ROMVP 5127**	**RLB *S. fatalis* ***	**Talara *S. fatalis* ***	***S. populator* ***
Length	81.45	82.46	90.6 ± 4.4	85.5 ± 1.1	89.2 ± 1.4
Shaft width	15.73	15.79	17.2 ± 0.5	16.5 ± 0.3	19.4 ± 0.4
Distal width	22.83	23.18	24.8 ± 0.8	24.3 ± 0.3	26.6 ± 0.2

* = Data from Kurtén & Werdelin, 1990

METACARPAL III	**ROMVP 5124**	**ROMVP 5128**	**RLB *S. fatalis* ***	**Talara *S. fatalis* ***	***S. populator* ***
Length	92.3	92.99	96.4 ± 4.0	97.3 ± 0.9	97.3 ± 2.7
Shaft width	14.87	15.23	17.3 ± 0.8	16.4 ± 0.3	19.4 ± 0.7
Distal width	23.2	23.78	26.5 ± 1.0	25.6 ± 0.4	28.2 ± 0.2

Transparent Methods

In 1961, A. G. Edmund and R. H. Lemon of the Royal Ontario Museum (ROMVP, Toronto, Ontario, Canada) collected and catalogued 4,231 specimens from a multitaxic bonebed at the Coralito locality (Spillmann, 1931) on the Santa Elena Peninsula of Ecuador (Figure 1). The locality is Lujanian in age (800 – 10 kya) and was first documented by Spillmann in 1931 (Spillmann, 1931). Unfortunately, detailed sedimentological and stratigraphic information for the locality were not collected during the ROM excavations, and the site has since undergone development and is now inaccessible (Lindsey and Seymour, 2015). Therefore, the geological information reported here has been compiled from field notes, the published literature, and new analyses on samples of matrix from the site. These sediment samples were collected from the interior of the *Smilodon fatalis* braincase, ROMVP 5099. To quantify sediment type, grain size, and maturity, samples were viewed and measured on an Olympus BX53M petrographic microscope using Stream Motion 2.2.

Identifications of the Coralito fossil bones were made using comparative material held in the ROMVP collection and the literature (Kurtén and Werdelin, 1990; Merriam and Stock, 1932; Shaw and Tejada-Flores, 1985). All measurements reported here were collected by ARR or KLS using calipers or taken from the literature where indicated. Weathering and abrasion were scored by ARR following Behrensmeyer (Behrensmeyer, 1978), and Voorhies Groups were determined following Voorhies (Voorhies, 1969). Bones were also inspected for signs of scavenging, gnaw marks, and other taphonomic signatures. Body mass was estimated using two metrics: the length of the lower carnassial, M_1, following Van Valkenburgh's (Van Valkenburgh, 1990) regression for felids; and the circumference of the femur following Christiansen & Harris (Christiansen and Harris, 2005). All estimates were corrected using developmental mass extrapolation (DME),

which accounts for the ontogenetic limb scaling patterns within a species (Erickson and Tumanova, 2000). The circumference of the largest femur from Talara, Peru (ROMVP 2332) was used as the reference adult in the DME calculation. The sexes of the two dentaries were estimated by determining the ratio of the M_1 crown length to total dentary length, and comparing these results to those obtained for Rancho La Brea specimens by Christiansen & Harris (Christiansen and Harris, 2012).

Systematic Palaeontology of Specimens

Order	Carnivora Bowdich 1821
Suborder	Feliformia Kretzoi 1945
Family	Felidae Fischer von Waldheim 1817
Subfamily	Machairodontinae Gill 1872
Genus	*Smilodon* Lund 1842
	Smilodon fatalis Leidy 1868

Referred Material – ROMVP 5099, incomplete cranium with braincase, right squamosal and glenoid; ROMVP 5100, complete left dentary with complete C_1, incomplete P_3 (roots), incomplete P_4 (distal half), and complete M_1; ROMVP 5101, complete left dentary with complete C_1 and complete M_1; ROMVP 5102, complete right premaxilla with complete I^2 and complete I^3; ROMVP 5103, complete right P^3; ROMVP 5104, incomplete right scapula, glenoid region only; ROMVP 5105, incomplete left scapula, glenoid region only; ROMVP 5106, incomplete right humerus, proximal epiphysis unfused and missing; ROMVP 5107, incomplete left ulna, both epiphyses unfused and missing; ROMVP 5108, complete right ulna; ROMVP

5109, complete left radius, epiphyses unfused; ROMVP 5110, complete left scapholunar; ROMVP 5111, incomplete right scapholunar, minor damage to the magnum articular surface; ROMVP 5112, complete right unciform; ROMVP 5113, complete right pisiform; ROMVP 5114 incomplete right innominate, lacking pubic and symphyseal regions; ROMVP 5115, incomplete right femur, epiphyses unfused and trochanter epiphysis missing; ROMVP 5116, incomplete left femur, epiphyses unfused and distal epiphysis missing; ROMVP 5118, incomplete left astragalus, proximal articular surface broken; ROMVP 5119, complete right navicular; ROMVP 5120 A, complete left proximal phalanx, manual digit IV; ROMVP 5120 B, complete left proximal phalanx, manual digit II; ROMVP 5120 C, complete right proximal phalanx, manual digit II; ROMVP 5121 A, complete right middle phalanx, pedal digit V; ROMVP 5121 B, complete right middle phalanx, pedal digit IV; ROMVP 5121 C, complete left middle phalanx, pedal digit V; ROMVP 5122, complete left distal ungual phalanx, possibly from manual digit III; ROMVP 5123, complete left metacarpal II; ROMVP 5124, complete left metacarpal III; ROMVP 5125, incomplete left metacarpal IV, proximal two-thirds; ROMVP 5126, complete left metacarpal V; ROMVP 5127, complete right metacarpal II; ROMVP 5128, complete right metacarpal III; ROMVP 5129, complete right metacarpal IV; ROMVP 5130; complete right metatarsal II; ROMVP 5131, incomplete left rib IV or V, epiphysis and distal end missing; ROMVP 5132, incomplete atlas/cervical vertebra I; ROMVP 5133, incomplete axis/cervical vertebra II, posterior epiphysis missing; ROMVP 5134, incomplete cervical vertebra III, anterior and posterior centrum epiphyses missing; ROMVP 5135, incomplete cervical vertebra IV, anterior and posterior centrum epiphyses missing; ROMVP 5136, incomplete cervical vertebra VI, anterior and posterior centrum epiphyses missing; ROMVP 5137, incomplete thoracic vertebra, centrum only; ROMVP 5139, incomplete thoracic vertebra XIII, anterior and posterior

centrum epiphyses missing; ROMVP 5140, incomplete lumbar vertebra I, anterior and posterior centrum epiphyses and metapophyses missing; ROMVP 5141, incomplete lumbar vertebra II, anterior and posterior centrum epiphyses and all processes missing; ROMVP 5142, incomplete lumbar vertebra III, anterior and posterior epiphyses and all processes missing; ROMVP 5143, incomplete lumbar vertebra IV, anterior and posterior epiphyses missing; ROMVP 5144, incomplete lumbar vertebra V, anterior and posterior epiphyses missing; ROMVP 5145, incomplete lumbar vertebra VI, anterior and posterior epiphyses missing; ROMVP 5146, incomplete lumbar vertebra VII, anterior and posterior epiphyses missing; ROMVP 61716, incomplete right proximal phalanx, manual digit IV; ROMVP 61717, incomplete rib VI?, epiphysis and most of shaft missing; ROMVP 19296, complete right ectocuneiform; ROMVP 19297, complete left trapezoid; ROMVP 19309, incomplete thoracic vertebra VII, anterior and posterior epiphyses missing, neural spine broken.

Description of Material

Skull

The skull is represented by a right premaxilla (ROMVP 5102) and a braincase with a partial right zygomatic arch (ROMVP 5099). The ascending plate and palatine process of the premaxilla is incomplete. The anterior margin and part of the lateral margin of the anterior palatine foramen are included in the premaxilla. Approximately one half of the lateral part of the premaxilla contributes to the alveolus of the upper canine. Two longitudinal ridges are visible on the ventral side of the premaxilla and are more prominent than those seen in *Panthera onca*. The

lateral ridge is more prominent than in *Smilodon populator* (ROMVP 411) and *Homotherium* and is consistent with this feature in *S. fatalis* from the nearby locality of Talara, Peru.

The portion of the braincase that is preserved is the posterior end, extending from just anterior to the optic nerve. The left zygomatic arch has been broken off at its base and the right zygomatic arch has been broken just after the lateral expansion of the squamosal turns anteriorly. In posterior view, the dorsal margin of the occiput is broad and rounded as in *Smilodon fatalis* from Rancho La Brea and Talara. The occipital crest is more pronounced than in *Panthera* and the width of the zygomatic arch is relatively narrow compared with *P. atrox*. The posterior end of the zygomatic arch is inflected dorsoventrally compared to the same region in *P. atrox*, and the glenoid fossa is more ventrally positioned relative to the basisphenoid. In profile the sagittal crest is convex rather than straight or slightly concave as in *P. atrox* and lacks the upward inflection at the occiput seen in *P. onca*. The external auditory meatus is tubular and is enclosed on its ventral side by the mastoid process. The lambdoid crest does not form a distinct angle where it meets the mastoid process, as in *S. populator*, and is rather in the same plane as the mastoid process as in *S. fatalis* (Kurten and Werdelin, 1990).

Upper Dentition

The right I^2 and I^3 are present in the premaxilla (ROMVP 5102), as well as an isolated right P^3 (ROMVP 5103). All three teeth show minimal wear. Both incisors are strongly recurved and possess distinct accessory cusps mesially and distally on their buccal margin. The main cusps on I^2 and I^3 are longer and more pointed than in *Panthera*. However, these are more gracile than in *Smilodon populator*, *Homotherium*, or *Xenosmilus*. The P^3 has both anterior and posterior accessory present, as well as a small tubercle on the distobuccal edge of the tooth. The P^3 is less

robust than in *P. atrox*, but is not vestigial as in *Xenosmilus* and is more robust than in *Homotherium*.

Dentary

Two left dentaries of remarkably similar size (ROMVP 5100 and ROMVP 5101) are preserved. The anterior face of the ramus has two and three foramina in ROMVP 5100 and ROMVP 5101, respectively. The lateral flanges are short, stopping above the ventral border of the dentary below the cheek teeth in ROMVP 5100, and ending at the same level as the ventral border in ROMVP 5101. The anterior edge of the flange is expanded more laterally in ROMVP 5101 than in ROMVP 5100, but both are more laterally expanded overall than in homotherin taxa. In neither specimen is the flange thin, as described for older individuals in Merriam and Stock (1932). There is a single, large mental foramen in both specimens as in *Smilodon fatalis* and *S. populator*, rather than two as in *S. gracilis*, *Panthera*, *Homotherium*, and *Xenosmilus*. In both dentaries, the coronoid processes are shorter and narrower anteroposteriorly at the base than in *Panthera*. The coronoid processes are angled more toward the posterior end than in *Xenosmilus* and are narrower anteroposteriorly at the dorsal end than in *Homotherium serum*. In dorsal view, the ventral margin of the dentary is concave beneath the masseteric fossa as in *Smilodon fatalis*. The mandibular condyle does not extend as far medially as the condyle in *P. atrox*. The angular process is broken in ROMVP 5100, but in ROMVP 5101 it is more prominently hooked medially than in *S. populator*, *Panthera,* or the homotherins.

Lower Dentition

ROMVP 5100 possesses a C_1, in situ roots from the P_3, partial P_4, and M_1 and ROMVP 5101 includes a C_1, M_1, and associated P_3. Both canines have carinae on the mesial and distal sides, the former of which terminates basally in a small cusp. These canines are less robust and more strongly recurved than in *Panthera*, *Homotherium*, or *Xenosmilus*. The P_3 associated with ROMVP 5101 has two roots that are in close association with one another and do not split until approximately 5 mm below the cementoenamel junction. The crown is much smaller than the same tooth in *Panthera*. It is interesting that both individuals possess a P_3, as this tooth was only present in 6% of mandibles assessed by Merriam and Stock (1932), and 4.76% (n=21) of *S. fatalis* mandibles from Talara, Peru. Only the posterior accessory cusps and both roots are preserved in the P_4 of ROMVP 5100. This tooth is tilted backward as in other machairodontine felids. The M_1 is also tilted backward in both specimens but is larger in ROMVP 5101 than in ROMVP 5100. Accessory cusps are present on both the mesial edge of the paraconid blade and the distal edge of the protoconid blade in both specimens; however, these are more pronounced in ROMVP 5101.

Cervical Vertebrae

The atlas and axis are preserved, as are the third, fourth, and sixth cervical vertebrae. The atlas (ROMVP 5132) is nearly complete but the left transverse process has been restored on the lateral edge. The transverse processes extend well beyond the posterior margin of the postzygapophyses and are tapered posteriorly and ventrally deflected as in *Smilodon fatalis*. The tubercle for the *longus colli* on the posteroventral surface of the body is not as pronounced as in *Panthera* or *Homotherium.* The axis (ROMVP 5133) is lacking the posterior epiphysis for the body and is slightly broken at the posterior ends of the neural spine and transverse processes.

The neural spine projects forward in line with the anteriormost part of the prezygapophyses and around 2 cm posterior to the postzygapophyses, as in *Smilodon*. The posterior end of the neural spine expands laterally, but does not inflect as strongly dorsally and remain pointed dorsally as in in *S. populator*. There is a median ridge along the ventral wall of the neural canal, which is expressed more prominently in this specimen than in extant *Panthera*.

Cervical vertebrae III (ROMVP 5134), IV (ROMVP 5135), and VI (ROMVP 5136) each lack both anterior and posterior epiphyses of the body and the distal ends of the transverse processes. The posterior end of the neural spine in cervical vertebra III is not inflected dorsally relative to the anterior end of the spine, as in *Smilodon fatalis* rather than *Panthera* or *S. populator*. Two small foramina are present on the lateral walls of the pedicle but without a depression as described in *P. atrox* by Merriam and Stock (1932). Cervical vertebra IV is lacking much of the neural spine, as is cervical vertebra VI in addition to much of the costal elements in the latter. The hyperapophyses in cervical vertebra IV, while damaged, are clearly more well-pronounced than in *Panthera tigris*. The lateral sides of the pedicles of both cervical vertebrae IV and VI do not have a marked depression as in *Panthera*. The costal elements of cervical vertebra VI project more ventrally than in *Panthera*.

Thoracic Vertebrae

Two thoracic vertebrae are preserved: VII (ROMVP 19309) and XIII (ROMVP 5139). Both specimens are lacking the anterior and posterior epiphyses of their centra and have broken neural spines. The right metapophysis and anapophysis are broken in ROMVP 5139. The ventral ridge described in Merriam and Stock (1932) is not present on the centrum of this vertebra, but this may be due to the incomplete development of the vertebra, weathering, or both. The anterior

edge of the surface below the metapophysis is very convex anteriorly as in *Smilodon* rather than *Panthera*.

Lumbar Vertebrae

A full lumbar series is present (I, ROMVP 5140; II, ROMVP 5141; III, ROMVP 5142; IV, ROMVP 5143; V, ROMVP 5144; VI, ROMVP 5145; VII, ROMVP 5146). All seven vertebrae are lacking the anterior and posterior epiphyses of the centrum. Lumbar vertebrae I, IV, and VI have complete neural spines, all of which have anterior edges that project almost straight dorsally, although slightly more so in I and IV. The distal end of the neural spine in VI is less flat than in *Panthera atrox*. The metapophyses are broken or worn at the prezygapophysis in all specimens. The median ventral ridge typical of *Smilodon* lumbar vertebrae is present in all specimens, but is only especially prominent in II-VII. Lumbar vertebra VI has deep grooves on the anterior face extending from the lateral ends of the neural canal to the bases of the transverse processes, much like in *S. fatalis* from Rancho La Brea. In lumbar vertebra VII, the metapophysis projects more directly dorsally than in *Panthera atrox*.

Ribs

Two ribs are preserved: one left (likely IV or V; ROMVP 5131) and one right (likely VII or VIII; ROMVP 61717 not sure about this one being right over left), both of which are missing the epiphysis of the head. ROMVP 5131 is almost complete, except for some missing chunks of bone between the dorsal crest and angle. ROMVP 61717 consists of only a head, neck, and tubercle. Both ribs are more robust than in *Panthera tigris*, with the shaft staying very robust throughout in ROMVP 5131.

Scapula

The glenoid regions of the right (ROMVP 5104) and left (ROMVP 5105) scapulae are preserved. The glenoid cavity of ROMVP 5105 is slightly damaged on its medioposterior border. The glenoid cavity is relatively narrower mediolaterally than in *Panthera atrox*. The glenoid cavity is deeper than in *Homotherium*, and the glenoid and neck are thicker medio-laterally.

Humerus

A single right humerus (ROMVP 5106), missing the proximal epiphysis and part of the medial condyle and trochlea, was recovered. Considering the missing epiphysis, it appears the specimen would have been approximately the same length as in *Panthera tigris*. The pectoral and deltoid ridges are not well-developed in this specimen, possibly due to the relatively young age of the individual as indicated by incomplete epiphyseal fusion. However, a larger sub-adult from the Talara deposits in Peru (ROMVP 3994) is also lacking the proximal epiphysis but has these ridges more prominently developed. The bone enclosing the entepicondylar foramen is narrower anteroposteriorly than in *P. atrox*. The lateral supracondylar ridge is straighter in anterior view than the same feature in *P. atrox*. The shaft is thicker than in *Homotherium*, with a broader capitellum medio-laterally.

Ulna

Two ulnae were recovered from Coralito. The first, ROMVP 5107, is a left element that is lacking the distal and olecranon epiphyses. The second, ROMVP 5108, is a complete adult right ulna that is substantially larger than ROMVP 5107 and is more deeply tar stained. Both

ulnae are bowed less laterally and anteriorly than in *Panthera atrox* or *Homotherium*. The distal end is much more robust than in *Homotherium*. The attachment area for the outer humeral head of the *triceps* extends further distally – at approximately the midpoint of the greater sigmoid cavity – in both specimens than in *P. atrox*, but not as far distally as in *S. populator*, in which the muscle attachment terminates at the distal end of the greater sigmoid cavity. ROMVP 5108 is greater in length than the largest ulna from Talara, and within the range but above the mean reported in Merriam and Stock (1932). The proximal end of the olecranon of ROMVP 5108 is wider than in *P. atrox*. Although nearly equal in length to the ulna of *S. populator*, ROMVP 5108 is less robust.

Radius

This assemblage includes a left radius (ROMVP 5109) with the distal epiphysis unfused but preserved, and a right radial epiphysis (ROMVP 77624). The tubercle for attachment of the *biceps* is not at defined distally and is oriented more laterally than in *Panthera atrox*. However, it is more protuberant than in *Homotherium*. The styloid process is stouter and the groove for the *extensores carpi radialis* and *brevior* is more pronounced than in *P. atrox*. The articular facet for the scapho-lunar is narrower mediolaterally but broader anteroposteriorly than in the lion.

Carpals

A left scapho-lunar (ROMVP 5110), right scapholunar (ROMVP 5111), right pisiform (ROMVP 5113), left trapezoid (ROMVP 19297), and right unciform (ROMVP 5112). The process on the radio-palmar side of the scapho-lunar is more elongate than in *Panthera atrox*. A notch on the palmar border of the articulation with the magnum is present in both scapho-lunars,

but this is more apparent in ROMVP 5111. The pisiform has a narrow head and wide shaft as in *S. fatalis*, with an articular surface for the ulna that does not project as far up the shaft as in *P. atrox*. The ridge along the articulation for the scapholunar on the proximal side of the trapezoid is not as sharp as in *P. atrox*. The proximodistal width of the palmar side of the unciform is relatively large, as in *S. fatalis*. A deeper depression is found on the palmar side of the articulation for the cuneiform than in *P. atrox*. On the distal side of the unciform, the articulation for metacarpal IV is transversely wider than that for metacarpal V.

Metacarpals

On the left side, metacarpals II (ROMVP 5123), III (ROMVP 5124), IV (ROMVP 5125), and V (ROMVP 5126) are preserved. Right metacarpals II (ROMVP 5127), III (ROMVP 5128), and IV (ROMVP 5129) are likewise present. The left side metacarpals articulate with each other well, as do metacarpals II and III on the right side. For all elements in which it is preserved, the palmar keel of the distal articulation is pronounced. In dorsal view, the proximal end of the metacarpal II is indented more pronouncedly than in *Panthera atrox*, and the tubercle distal to the groove for the radial artery is more protuberant. The articular facet for the trapezium is elongated proximo-distally and projects proximally beyond the proximal border of the element. On the lateral side, there is no visible articular surface for the magnum and the dorsal articulation for the metacarpal III is less deeply grooved than in *P. atrox*. The depression on the dorsal surface of the distal end of the shaft, just before the distal epiphysis, extends farther proximally than in the lion. Both metacarpals III widen from their proximal to distal ends in dorsal view. In medial or lateral view, the proximal end is not as wide in the dorso-palmar plane as in *P. atrox*. In proximal view, the articular facet for the magnum is distinctly notched on the medial side. An

articular facet is present on the proximo-lateral side as in *Smilodon fatalis*. The left metacarpal IV is broken mid-shaft. The proximal end of this element is not as deeply notched on the lateral side as in *P. atrox*. On metacarpal V, the articulation with metacarpal IV is not as large as in *P. atrox*, with a broader notch between the dorsal and palmar surfaces of this facet. The tuberosity on the lateral side of the proximal end is indented along a dorso-palmar plane. There is a distinct ridge separating the medial and palmar surfaces of the shaft.

Innominate

A right innominate (ROMVP 5114), lacking the pubic and symphyseal regions, is preserved. The epiphyses of the iliac crest and tuberosity of the ischium do not appear to be fused. The depression on the lateral surface of the illium is less deep than in *Panthera atrox*. The region of attachment with the sacrum on the inner aspect is rugose. The areas of attachment for the *rectus femoris* and *gluteus quartus* muscles are prominent as in *S. fatalis*. The articular surface for the acetabulum is broader than in *P. atrox*.

Femur

The right femur (ROMVP 5115) is a diaphysis with free head and distal epiphyses. The left femur (ROMVP 5116) consists of the diaphysis with free head and trochanter epiphyses. In lateral or medial view, the diaphysis appears flatter posteriorly than in *Panthera atrox*. The diaphysis is slenderer, particularly proximally, than in *Homotherium*. The trochanteric fossa is not as deep as in *P. atrox*, and the posterior side is more prominently pointed proximally than in *Homotherium*. There is a prominent, rounded tuberosity on the postero-lateral side of the neck, as in *Smilodon fatalis*. The lateral border of the patellar surface projects further anteriorly than

the medial border; the two borders are approximately equal in anterior extent in *Homotherium and P. atrox*. The medial condyle projects further posteriorly than in *Homotherium*.

Tarsals

The left astragalus (ROMVP 5118), right navicular (ROMVP 5119), and right ectocuneiform (ROMVP 19296) were found at Coralito. The trochlear surface of the astragalus is divided in two relatively equal halves, rather than the subequal division in *Panthera atrox*. This trochlear facet is broader than in *Homotherium*. The tibial side of the head is hooked proximally on the palmar side as in *Smilodon*. As in machairodontines, the navicular lacks a tuberosity on the plantar-proximal side. It is wider in the plantar-dorsal plane than in *Homotherium* and the articular facet for the ectocuneiform is more triangular. The ectocuneiform is of the truncated morphology described by Merriam and Stock (1932) and Shaw and Tejada-Flores (1985), which is considerably rarer in the Rancho La Brea population of *S. fatalis* compared with the Talara population. The groove for the tendon of the *peroneus longus* is deeper than in *Homotherium*. The proximal side of this groove is bifurcated toward the tibial and fibular sides; this bifurcation is not seen in *Homotherium* or *Panthera*.

Metatarsals

The metatarsal II (ROMVP 5130) is much shorter and wider medio-laterally than in *Homotherium*, with its lateral edge more rounded than in the homotherin. The lateral facets for the ectocuneiform extend to the proximal end of the bone, where the articulation for the mesocuneiform is narrower than in *Panthera atrox*.

Phalanges

Three proximal phalanges (ROMVP 5120 A [left manus, digit IV], B [left manus, digit II], and C [right manus, digit II]), three middle phalanges (ROMVP 5121 A [right pes, digit V], B [right pes, digit IV], and C [left manus, digit V]), and a left ungual phalanx (ROMVP 5122 [possibly left manus, digit III]) are preserved.

Supplemental References

Behrensmeyer, A.K., 1978. Taphonomic and ecologic information from bone weathering. Paleobiology 4, 150–162. https://doi.org/10.1017/s0094837300005820

Bowdich, T.E., 1821. An analysis of the natural classifications of Mammalia, for the use of students and travelers. J. Smith, Paris, France.

Christiansen, P., Harris, J.M., 2012. Variation in Craniomandibular Morphology and Sexual Dimorphism in Pantherines and the Sabercat *Smilodon fatalis*. PLoS One 7, e48352. https://doi.org/10.1371/journal.pone.0048352

Christiansen, P., Harris, J.M., 2005. Body Size of *Smilodon* (Mammalia: Felidae). J. Morphol. 266, 369–384. https://doi.org/10.1002/jmor.10384

Erickson, G.M., Tumanova, T.A., 2000. Growth curve of Psittacosaurus mongoliensis Osborn (Ceratopsia: Psittacosauridae) inferred from long bone histology. Zool. J. Linn. Soc. 130, 551–566. https://doi.org/10.1006/Zjls.2000.0243

Fischer von Waldheim, G., 1817. Adversaria Zoologica, fasciculus primus. Mémoires la Société des Nat. Moscou 5, 357–446.

Gill, T., 1872. Arrangement of the families of mammals. With analytical tables. Smithson. Misc. Collect. 230, 1–348.

Kretzoi, M., 1945. Bemerkungen über das Raubtiersystem. Ann. Hist. Musei Natl. hungarici 38, 59–83.

Kurtén, B., Werdelin, L., 1990. Relationships between North and South American *Smilodon*. J. Vertebr. Paleontol. 10, 158–169.

Leidy, J., 1868. Notice of some vertebrate remains from Harden Co., Texas. Proc. Acad. Nat. Sci. Philadelphia 20, 174–177.

Lindsey, E.L., Seymour, K.L., 2015. "Tar Pits" of the Western Neotropics: Paleoecology, Taphonomy, and Mammalian Biogeography, in: Harris, J.M. (Ed.), La Brea and Beyond: The Paleontology of Asphalt-Preserved Biotas, Natural History Museum of Los Angeles County Science Series No. 42. Allen Press, Inc., Los Angeles, California, pp. 111–123.

Lund, P.W., 1842. Blik paa Brasiliens dyreverden för sidste jordomvaeltning. Fjerde afhandling: fortsaettelse af pattedyrene. Saerskilt afteyet af det K. Danske Vidensk. Selsk. Naturvidenskabelige og Mat. Afh. 1–72.

Merriam, J.C., Stock, C., 1932. The Felidae of Rancho La Brea. Carnegie Institution of Washington, Publication 422.

Shaw, C.A., Tejada-Flores, A.E., 1985. Biomechanical implications of the variation in Smilodon ectocuneiforms from Rancho La Brea. Los Angeles Cty. Museum Contrib. Sci. 359, 1–8.

Spillmann, F., 1931. Die Säugetiere Ecuadors im Wandel der Zeit. Universidad Central, Quito, Ecuador.

Van Valkenburgh, B., 1990. Skeletal and dental predictors of body mass in carnivores, in: Damuth, J., MacFadden, B.J. (Eds.), Body Size in Mammalian Paleobiology: Estimation and Biological Implications. Cambridge University Press, Cambridge, UK, pp. 181–205.

Voorhies, M.R., 1969. Taphonomy and population dynamics of an early Pliocene vertebrate

fauna, Knox County, Nebraska. Univ. Wyoming Contrib. to Geol. Spec. Pap. No. 1 69 pp. https://doi.org/10.2113/gsrocky.8.special_paper_1.1